Inorg. Chem. **2003**, *42*, 7315–7318

Synthesis, Structure, and Magnetoresistance of $SmPd_2Ga_2$

Willa M. Williams,[†] Robin T. Macaluso,[†] M. Moldovan,[‡] D. P. Young,[‡] and Julia Y. Chan*[,†]

Department of Chemistry, Louisiana State University, Baton Rouge, Louisiana 70803, and Department of Physics and Astronomy, Louisiana State University, Baton Rouge, Louisiana 70803

Received June 12, 2003

Single crystals of a new ternary compound, $SmPd_2Ga_2$, have been synthesized by flux growth methods. This compound adopts a tetragonal space group *I*4/*mmm*, $Z = 2$, with lattice parameters $a = 4.2170(3)$ Å and $c = 10.4140(3)$ Å. The crystal structure is composed of layers of isolated Sm atoms and layers of $PdGa_4$ edge-sharing tetrahedra alternating along the *c*-axis. The sample is metallic ($d\rho/dT > 0$) with a weak temperature dependence above 100 K. This new material has physical properties similar to those of other Sm intermetallics and has, most notably, a large positive magnetoresistance at low temperatures. Magnetic measurements indicate that $SmPd_2Ga_2$ is ferromagnetic with $T_c \sim 5$ K.

Introduction

Compounds of the $ThCr_2Si_2$-structure type are abundant due to their robust structure and the interesting physical properties that result from the ability of this structure to adopt different elements with various atomic sizes.[1−4] A significant number of these compounds have been shown to exhibit superconductivity, including the well-known Ln−Ni−B−C (Ln = lanthanide), which are stuffed variants of the $ThCr_2Si_2$-structure type.[5] Other compounds boast a wide range of magnetic properties. UCr_2Si_2 and $PrNi_2Ge_2$ order antiferromagnetically at $T_N = 210$ K and $T_N = 24$ K, respectively,[6] and $EuNi_2P_2$ is an interesting compound because of the mixed valence states of Eu(2+/3+).[7] Several ternary Ln−Pd−Ga-containing phases are known to adopt the $BaAl_4$ structure type which is related to the $ThCr_2Si_2$-structure type when $x = 2$ in $LnPd_xGa_{4-x}$. Ternary gallides (La, Ce, Pr, Nd, Sm)Pd_xGa_{4-x} have been shown to exhibit solid solutions in arc-melted samples of $LnPd_xGa_{4-x}$ at various compositions.[8]

$LaPd_2Ga_2$ and $CePd_2Ga_2$ crystallize in the $CaBe_2Ge_2$-structure type and undergo a structural phase transition with decreasing temperature at 65 and 125 K, respectively.[9] The physical properties of this family of materials are also quite interesting and often display strongly correlated electron behavior. $LaPd_2Ga_2$ is a superconductor with a critical temperature of 1.9 K, while the Ce analogue orders antiferromagnetically at 2.3 K.[12] Compounds of the $ThCr_2Si_2$- and $CaBe_2Ge_2$-structure types share similar structural features. Both structures are described by tetragonal unit cells with comparable lattice parameters (~4 Å × 10 Å). The $CaBe_2Ge_2$ type (space group *P*4/*mmm*) is closely related to the $ThCr_2Si_2$ type (space group *I*4/*mmm*) and forms in the temperature range of 1100−1700 °C. In some cases, i.e., $EuZn_2Ge_2$, it is almost impossible to discriminate between the two structure types by X-ray diffraction.[9]

The structure type in RT_2X_2 compounds (R = lanthanide, T = transition metal or main group, X = main group element) is influenced by atomic radii and synthesis conditions of the constituent elements. The $CaBe_2Ge_2$ type is more prone to form when a sample is quenched at high temperatures.[10] The $CaBe_2Ge_2$ type consists of layers of edge-sharing $BeGe_4$ and $GeBe_4$ tetrahedra with alternating layers of isolated Ca atoms in a 1:1:1 ratio. In contrast, the $ThCr_2$-

* To whom correspondence should be addressed. E-mail: julia.chan@chem.lsu.edu. Telephone: (225) 578-2695. Fax: (225) 578-3458.
[†] Department of Chemistry.
[‡] Department of Physics and Astronomy.

(1) Bancroft, N. J.; Paul, D. M.; McIntyre, G.; Dewhurst, C. D. *Pramana* **2002**, *58*, 907.
(2) Barakatova, Z. M.; Kochetkov, Y. V.; Mirkovich, I.; Nikiforov, V. N. *Russ. Metall.* **1996**, 137.
(3) Bhan, S.; Kudielka, H. *Z. Metallkd.* **1978**, *69*, 333.
(4) Drzazga, Z.; Fuchs, G.; Handstein, A.; Nenkov, K. *Physica C* **2003**, *383*, 421.
(5) Elderman, Y.; Kervan, S.; Duman, E. *J. Magn. Magn. Mater.* **2002**, *251*, 251.
(6) Hillier, A. D.; Preston, J. M.; Stewart, J. R.; Cywinski, R. *Hyperfine Interact.* **2001**, *136*, 313.
(7) Hofmann, M.; Campbell, S. J.; Edge, A. V. J. *Appl. Phys. A* **2002**, *74*, S713.
(8) Grin, Yu N.; Rogl, P.; Hiebl, K.et. *J. Less-Common Met.* **1986**, *118*, 335.
(9) Kranenberg, C.; Johrendt, D.; Mewis, A.; Pottgen, R.; Kotzyba, G.; Trill, H.; Mosel, B. D. *J. Solid State Chem.* **2002**, *167*, 107.
(10) Kitagawa, J.; Ishikawa, M. *J. Phys. Soc. Jpn.* **1999**, *68*, 2380.
(11) Kranenberg, C.; Johrendt, D.; Mewis, A.; Pottgen, R.; Kotzyba, G.; Trill, H.; Mosel, B. D. *J. Solid State Chem.* **2002**, *167*, 107.
(12) Mewis, A. *Z. Anorg. Allg. Chem.* **1986**, *536*, 7.

10.1021/ic034660r CCC: $25.00
Published on Web 10/02/2003

Si_2 type consists of $CrSi_4$ edge-sharing tetrahedra with alternating layers of isolated Th atoms in a 1:1 ratio. Band structure calculations have shown that the $ThCr_2Si_2$ type is more stable at room temperature due to its less dispersed filled band and its lower Fermi level. A Monte Carlo simulation study showed that at high temperatures entropic contributions become more important and thus can favor the $CaBe_2Ge_2$ type.[11]

Intermetallic compounds containing Sm often exhibit unique magnetic behavior. This is often due to Sm ions existing in multiple electronic configurations ($4f^6$ and $4f^5$), which are referred to as mixed-valence systems. $SmPd_2Si_2$ shows evidence of spontaneous magnetism at temperatures below 34 K.[13] $Gd_{0.925}La_{0.075}Mn_2Ge_2$, which is isostructural to $SmPd_2Ga_2$, has been shown to exhibit negative magnetoresistance ($\Delta\rho/\rho_0 \sim 15\%$ at 145 K).[14] In our search for novel ternary intermetallics, we have discovered $SmPd_2Ga_2$, which also crystallizes in the $ThCr_2Si_2$-structure type. In this paper, we report the synthesis, crystal structure, and physical properties of $SmPd_2Ga_2$.

Experimental Section

Syntheses. The samples were synthesized from small chunks of Sm (99.9+%, Ames Laboratory), Pd powder (99.998%, Alfa Aesar), and Ga pieces (99.99999%, Alfa Aesar). Single crystals were grown by placing the constituent elements in an aluminum oxide crucible in a molar ratio of 1:1:20. The sample was sealed in an evacuated quartz tube and heated to a temperature of 1170 °C for 7 h and slowly cooled to 350 °C, at which point the hot flux was removed by centrifugation. Large crystals of $SmPd_2Ga_2$ were obtained and showed no signs of instability or degradation when exposed to air.

Single-Crystal X-ray Diffraction. A suitable crystal of ~0.02 mm × 0.08 mm × 0.02 mm was mechanically extracted, placed on a glass fiber, and mounted on the goniometer of a Nonius Kappa CCD diffractometer equipped with monochromated Mo Kα radiation ($\lambda = 0.701\ 73$ Å). Additional data collection parameters and crystallographic information are presented in Table 1.

The structure was solved using direct methods (SHELXL97).[13] Data were then corrected for extinction and refined with anisotropic displacement parameters. Atomic positions and related structural information is provided in Table 2. Selected interatomic distances and bond angles are given in Table 3.

Property Measurements. The electrical resistivity of a single crystal of $SmPd_2Ga_2$ was measured by the standard 4-probe ac technique at 27 Hz with a current of 1 mA. The 1-mil Pt wires were attached to the sample with silver epoxy. The magnetoresistance and magnetic susceptibility were measured in a 9-T PPMS system from Quantum Design.

Results and Discussion

Structure. The structure of $SmPd_2Ga_2$ is provided in Figure 1. $SmPd_2Ga_2$ is isostructural to $ThCr_2Si_2$ and crystallizes in the tetragonal *I*4/*mmm* space group (No. 139) with Sm, Pd, and Ga occupying the 2*a*, 4*d*, and 4*e* sites, respectively. The crystal structure consists of layers of $PdGa_4$ edge-sharing tetrahedra alternating with layers of isolated Sm atoms in a 1:1 ratio along the *c*-axis. Each Pd atom is coordinated to 4 Ga atoms by a bond distance of 2.514(5) Å, which is in agreement with the summation of the atomic radii of Ga (1.22 Å) and Pd (1.37 Å), as well as the typical interatomic distances in Pd−Ga binaries. In Pd_2Ga, for example, Pd and Ga atoms are separated by 2.558 Å. The Pd−Ga distances in Pd_5Ga_3 range between 2.388 and 2.701 Å and are 2.501−2.691 Å in $PdGa_5$ and Pd_2Ga.[15,16] Each layer of $PdGa_4$ tetrahedra is connected to the next layer of $PdGa_4$ tetrahedra by a 2.47(2) Å Ga−Ga bond along the *c*-axis. The Ga−Ga interatomic distance of 2.47(2) Å also agrees with the calculated value of 2.44 Å. The Ga−Ga interatomic distances agree with interatomic distances reported in $CeGa_6$, $CeGa_2$, and $PdGa_5$ which fall within the

Table 1. Crystallographic Parameters

Crystal Data	
formula	$SmPd_2Ga_2$
a (Å)	4.2170(3)
c (Å)	10.4140(3)
V (Å^3)	185.57
Z	2
crystal dimens (mm^3)	0.04 × 0.04 × 0.08
cryst system	tetragonal
space group	*I*4/*mmm*
θ range (deg)	1.0−27.48
μ (mm^{-1})	63.03
Data Collection	
measd reflcns	941
indpdt reflcns	144
reflcns with $I > 2\sigma(I)$	142
R_{int}	0.081
h	−5 → 5
k	−5 → 5
l	−14 → 14
Refinement	
$R_1[F^2 > 2\sigma(F^2)]$[a]	0.0424
$wR_2(F^2)$[b]	0.1156
reflcns	144
params	12
$\Delta\rho_{max}$ (e Å^{-3})	2.412
$\Delta\rho_{min}$ (e Å^{-3})	−1.023
extinction coeff	0.008(9)

[a] $R_1 = \Sigma||F_o| - |F_c||/\Sigma|F_o|$. [b] $wR_2 = \Sigma[w(F_o^2 - F_c^2)]/\Sigma[w(F_o^2)^2]^{1/2}$.

Table 2. Atomic Positions and Thermal Parameters of $SmPd_2Ga_2$

atom		x	y	z	U_{11}	U_{22}	U_{33}
Sm1	2*a*	0	0	0	0.0095(7)	0.0095(7)	0.0206(1)
Pd1	4*d*	0	1/2	1/4	0.0250(6)	0.0250(6)	0.0224(7)
Ga1	4*e*	0	0	0.38217(5)	0.0161(5)	0.0161(5)	0.0503(6)

Table 3. Selected Interatomic Distances and Bond Angles of $SmPd_2Ga_2$

param	interatomic dists (Å)
Sm1−Ga1 (×12)	3.227(4)
Sm1−Pd1 (×8)	3.350(2)
Within the $PdGa_4$ Tetrahedron	
Ga1−Pd1 (×4)	2.514(5)
Pd1-Pd1 (×4)	2.981(9)
Ga1−Ga1	2.47(2)
Param	**angles (deg)**
Ga1−Sm1−Ga1 (×2)	107.3(9)
Ga1−Sm1−Ga1 (×2)	113.7(3)

(13) Quebe, P.; Jeitschko, W. *J. Solid State Chem.* **1995**, *115*, 37.
(14) Fujiwara, T.; Fujii, H. *Phys. Rev. B* **2001**, *300*, 198.
(15) Sheldrick, G. M. *Acta Crystallogr., Sect. B: Struct. Sci.* **1998**, *54*, 443.
(16) Welter, R.; Venturini, G.; Malaman, B. *J. Alloy Compd.* **2001**, *329*, 69.

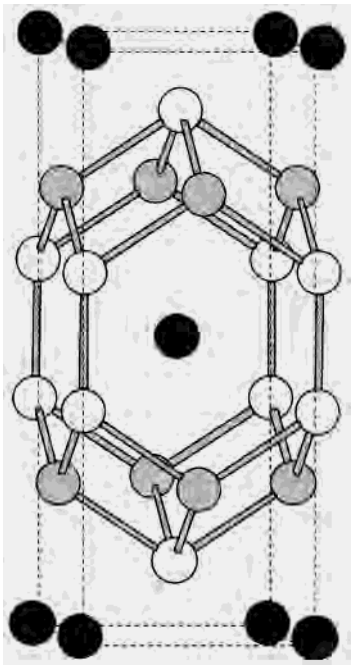

Figure 1. Crystal structure of (a) $SmPd_2Ga_2$ is shown along the *c*-axis. The Pd atoms are shaded dark gray, the body centered Sm atoms are shaded black, and Ga atoms are shown as white circles.

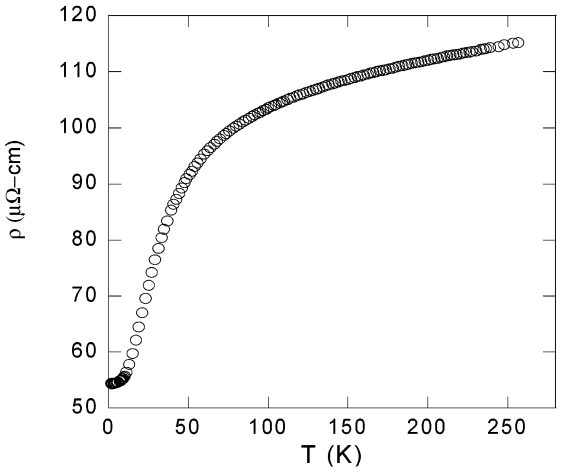

Figure 2. In-plane electrical resistivity of a single crystal of $SmPd_2Ga_2$ as a function of temperature.

range of 2.297−2.930 Å.[17,18] Ga−Pd−Ga bond angles in the $PdGa_4$ tetrahedron are 107.3(9) and 113.7(3)°, which are slightly distorted. The layers of $PdGa_4$ tetrahedra form a cagelike structure, which encapsulates one Sm atom. In the samarium layer, the Sm−Sm interatomic distance of 4.2170(3) Å is too long to be considered as bonding.

Physical Properties. The in-plane (*a*−*b*-plane) resistivity of a single crystal of $SmPd_2Ga_2$ as a function of temperature from 1.8 to 300 K is shown in Figure 2. The sample is metallic ($d\rho/dT > 0$) with a weak temperature dependence above 100 K. A broad shoulder occurs in the data near 60 K, and the resistivity decreases more rapidly below this temperature. This type of behavior is often observed in Kondo lattice systems in which the conduction electrons

(17) Zheng, C. *J. Solid State Chem.* **1988**, *72*, 58.
(18) Zheng, C. *J. Am. Chem. Soc.* **1993**, *115*, 1047.

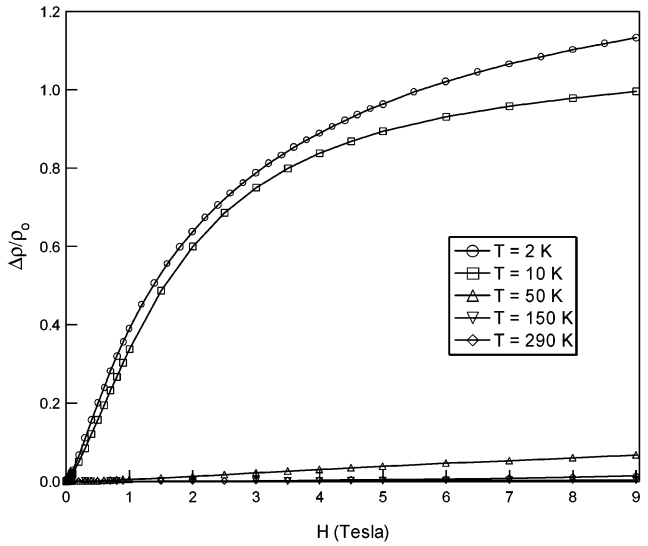

Figure 3. Relative in-plane magnetoresistance of a single crystal of $SmPd_2Ga_2$ at different temperatures with $H \parallel c$.

interact with local magnetic moments. The drop in the resistivity is usually associated with the onset of Kondo coherence. No superconductivity in $SmPd_2Ga_2$ was observed down to a temperature of 1.8 K.

The in-plane relative magnetoresistance (MR = $\Delta\rho/\rho_0$) of $SmPd_2Ga_2$ at different temperatures is shown in Figure 3, where $\Delta\rho = \rho(H) - \rho_0$ and $\rho_0 = \rho(0)$. The MR is positive and quite large at 2 K, increasing by over 100% at 9 T. In fact, the 9-T MR at 2 K is comparable to the zero-field resistivity at room temperature. The MR also appears to violate Kohler's rule, as the MR does not scale as a function of $F(H/\rho_0)$. The MR decreases with increasing temperature, and above 50 K, the MR is quickly suppressed. This occurs in the same temperature range where the broad shoulder appears in the zero-field resistivity. The large MR could be related to topological features of the Fermi surface, or it may result from an increase in spin-disorder scattering as suggested by magnetization data presented below. Measurements of the magnetization at low temperatures and high fields (de Haas van-Alphen effect) can be used to experimentally determine the Fermi surface, and such experiments are planned for the near future.

Figure 4 shows a plot of the magnetic susceptibility of a single crystal of $SmPd_2Ga_2$ taken in a magnetic field of 1000 G with the field oriented along the *c*-axis. The data are qualitatively consistent with a local moment system. However, the inverse susceptibility plotted versus temperature (not shown) is not linear at high temperatures, as would be expected for the Curie−Weiss law. The weaker than linear increase in the reciprocal susceptibility is consistent with Sm ions in the 3+ state in conjunction with a large temperature-independent van Vleck susceptibility. Such behavior is typical in Sm intermetallics. By using a modified Curie−Weiss law of the form: $\chi(T) = \chi_0 + C/(T - \Theta)$, we were able to fit the magnetic susceptibility data quite well down to ~8 K (see solid line, main panel of Figure 4). Here, χ_0 represents the temperature-independent van Vleck term, *C* is the Curie constant, and Θ is the Weiss temperature. By

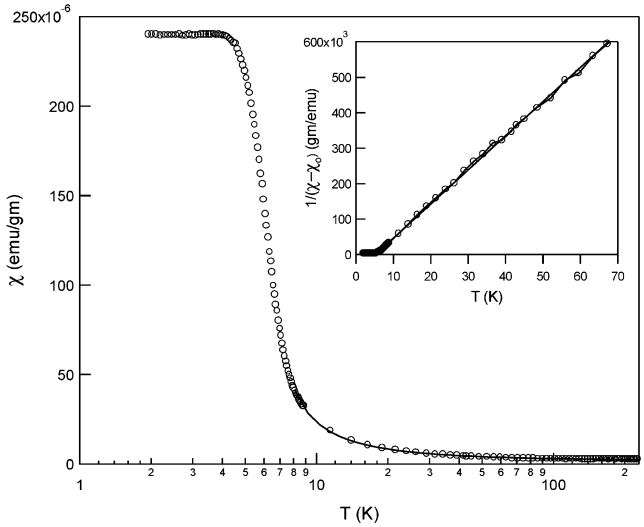

Figure 4. Temperature-dependent magnetic susceptibility ($\chi = M/H$) in a field of 1000 G with $H \| c$. Inset: Inverse susceptibility with van Vleck term subtracted versus temperature. The solid lines are fits to the data as described in the text.

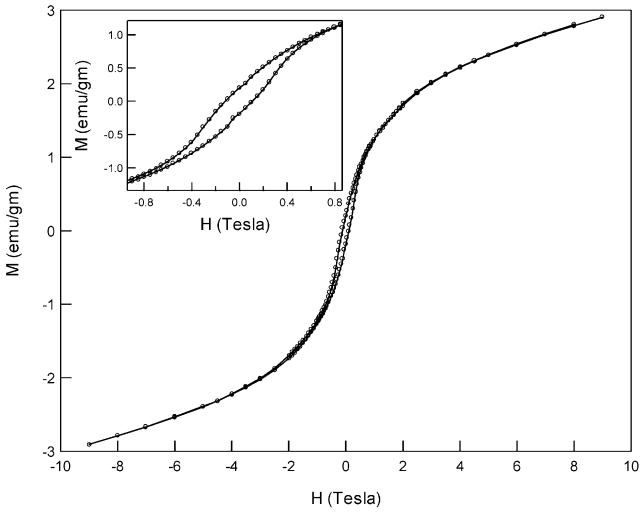

Figure 5. Magnetization versus applied field of a single crystal of $SmPd_2Ga_2$ for $H \| c$ and $T = 2$ K. The inset shows an expanded view of the low-field region, clearly showing hysteresis in the magnetization.

plotting the inverse susceptibility versus temperature with χ_0 subtracted from the raw data, we find linear behavior extending up to ~70 K (see inset Figure 4). From a linear fit to this curve we obtain values of 1.2×10^{-4} (emu K)/g and 5.2 K for C and Θ, respectively. The positive value of Θ suggests ferromagnetic correlations, and from C we calculate an effective magnetic moment $p = 0.70\ \mu_B$/mol Sm. This is smaller than, but close to, the full Hund's rule moment for Sm^{3+}.

Further evidence for ferromagnetic ordering is shown in Figure 5, where we plot the magnetization versus applied field at 2 K. The magnetization is not saturated, even at a field of 9 T, and the low-field data (inset Figure 5) clearly show hysteresis in the magnetization—a clear sign of ferromagnetism. Given that the MR at 2 K tends to track the magnetization, we feel an increase in the spin-disorder scattering is a plausible explanation for the large MR at low temperature.

In conclusion, we have synthesized the new ternary intermetallic $SmPd_2Ga_2$ by metal flux techniques and determined its crystal structure. The material forms in the $ThCr_2Si_2$ structure which is common for many RT_2X_2 compounds, where R is a lanthanide, T is a transition metal, and X is a group 3 or 4B element. $SmPd_2Ga_2$ is metallic and orders ferromagnetically at 5 K. It has an unusually large positive magnetoresistance at low temperatures that may be due to an increase in spin-disorder scattering. No superconductivity was observed down to 1.8 K.

Acknowledgment. This material is based upon work supported by the National Science Foundation Career Grant No. DMR-0237664 and ACS Petroleum Research Fund. D.P.Y. and J.Y.C. also acknowledges the Louisiana Board of Reagents for partial support for this project.

Supporting Information Available: Crystallographic data in CIF format for $SmPd_2Ga_2$. This material is available free of charge via the Internet at http://pubs.acs.org

IC034660R